Curcumin inhibits cystogenesis by simultaneous interference of multiple signaling pathways: in vivo evidence from a *Pkd1*-deletion model

Wouter N. Leonhard,[1] Annemieke van der Wal,[2] Zlata Novalic,[1] Steven J. Kunnen,[1] Ron T. Gansevoort,[3] Martijn H. Breuning,[1] Emile de Heer,[2] and Dorien J. M. Peters[1]

Departments of [1]Human Genetics and [2]Pathology, Leiden University Medical Center, Leiden; and [3]Division of Nephrology, Department of Internal Medicine, University Medical Center Groningen, Groningen, The Netherlands

Leonhard WN, van der Wal A, Novalic Z, Kunnen SJ, Gansevoort RT, Breuning MH, de Heer E, Peters DJ. Curcumin inhibits cystogenesis by simultaneous interference of multiple signaling pathways: in vivo evidence from a *Pkd1*-deletion model. *Am J Physiol Renal Physiol* 300: F1193–F1202, 2011. First published February 23, 2011; doi:10.1152/ajprenal.00419.2010.—Autosomal dominant polycystic kidney disease (ADPKD) caused by mutations in either the *PKD1* or *PKD2* gene is a major cause of end-stage renal failure. A number of compounds targeting specific signaling pathways were able to inhibit cystogenesis in rodent models and are currently being tested in clinical trials. However, given the complex signaling in ADPKD, an ideal therapy would likely have to comprise several pathways at once. Therefore, multitarget compounds may provide promising therapeutic interventions for the treatment of ADPKD. To test this hypothesis, we treated *Pkd1*-deletion mice with diferuloylmethane (curcumin), a compound without appreciable side effects and known to modulate several pathways that are also altered in ADPKD, e.g., mammalian target of rapamycin (mTOR) and Wnt signaling. After conditional inactivation of *Pkd1*, mTOR signaling was indeed elevated in cystic kidneys. Interestingly, also activation of signal transducers and activator of transcription 3 (STAT3) strongly correlated with cyst progression. Both pathways were effectively inhibited in vitro by curcumin. Importantly, *Pkd1*-deletion mice that were treated with curcumin and killed at an early stage of PKD displayed improved renal histology and reduced STAT3 activation, proliferation index, cystic index, and kidney weight/body weight ratios. In addition, renal failure was significantly postponed in mice with severe PKD. These data suggest that multitarget compounds hold promising potential for safe and effective treatment of ADPKD.

autosomal dominant polycystic kidney disease; signal transducers and activator of transcription 3; mammalian target of rapamycin; multitarget therapy

THE FORMATION AND PROGRESSION of thousands of cysts accompanied by progressive fibrosis in kidneys of autosomal dominant polycystic kidney disease (ADPKD) patients lead to renal failure, generally ~50–60 years of age. Extra renal manifestations that can occur in ADPKD are the formation of cysts in liver and pancreas, cardiovascular abnormalities, and hypertension (14). ADPKD has an incidence of 1 in 400 to 1 in 1,000 and is caused by either a mutation in the *PKD1* gene, encoding the protein polycystin-1 (PC1; 85% of clinical cases), or a mutation in the *PKD2* gene, encoding polycystin-2 (PC2; 15% of clinical cases) (42, 46, 62). A balanced expression of these genes is essential to maintain renal epithelial architecture (28, 48, 68).

Earlier we developed an inducible kidney-specific *Pkd1*-deletion (iKsp-*Pkd1*^del) mouse model in which we can inactivate the *Pkd1* gene specifically in renal epithelial cells by the administration of tamoxifen (29, 30). When *Pkd1* is inactivated at postnatal (PN) *day 40*, cystogenesis takes place and is followed by renal failure 13–16 wk after tamoxifen administration. These iKsp-*Pkd1*^del mice do not have extra renal manifestations and can serve as a model for testing therapeutic interventions for the treatment of ADPKD.

This and other ADPKD model systems have been utilized to study the functions of the PKD genes. Although not exactly known, a wealth of literature exists that ascribes roles for both polycystins in regulating signaling pathways that control proliferation, differentiation, and planar cell polarity (PCP), mechanosensation, cell-cell and cell-matrix interactions (7, 18, 43, 54, 67). Among others, increased cAMP, decreased intracellular calcium levels, altered mammalian target of rapamycin (mTOR), and Wnt signaling and abnormal chloride-driven fluid secretion via the cystic fibrosis transmembrane conductance regulator channel all seem to contribute to cyst formation and progression (18, 27, 34, 41, 55, 56, 61, 64, 65). Furthermore, additional triggers like tubular kidney damage drastically accelerate cystogenesis (18, 60).

Although multiple pathways are involved in ADPKD, compounds that have been reported to inhibit cystogenesis and are currently being investigated in clinical trials mostly act on single pathways (6, 19, 45, 63). Their specificity compels them to be used at relative high dosages that consequently have adverse implications regarding side effects. Therapies that simultaneously interfere with a wider spectrum of PKD-related pathways may therefore be more successful and should be evaluated as candidates for the treatment of ADPKD.

The polyphenol diferuloylmethane (curcumin) is a yellow spice derived from the rhizome of the plant Curcuma Longa (26). Its anti-oxidant, anti-inflammatory, and anti-proliferative properties initiated many studies for the treatment of several diseases. Curcumin has been shown to be safe and effective in treating several inflammatory and malignant diseases in animal models and, although preliminary, also in a number of early phase clinical trials (3, 12, 16, 22, 24, 58, 59). In addition, promising developments regarding curcumin analogs and other multitarget compounds will likely improve their utility in clinical settings (1, 20, 21, 25, 36, 39, 40, 57). The complex mechanisms by which curcumin exerts its beneficial effects involve a wide variety of pathways (26, 58). Inhibition has been reported for the transcription factors activator protein-1, nuclear factor-κB (NF-κB), Wnt/β-catenin signaling, TNF-α, MAPKs, early growth response gene-1, hypoxia inducible factor-1, notch-1, and also the mTOR-regulated signaling (4, 5,

23, 26, 32, 58). Many of these pathways are altered in ADPKD (27, 31, 35, 55, 56, 61, 69). In addition, curcumin acts as a free radical scavenger and may further attenuate several forms of tubular injury by induction of NF-E2-related factor-2 (Nrf2) and subsequent increase of several cytoprotective enzymes (2). The ability of curcumin to inhibit signal transducer and activator of transcription 3 (STAT3) may also be relevant to ADPKD since we show here that STAT3 is activated in iKsp-$Pkd1^{del}$ mice (10, 26).

The similarities between altered signaling pathways in ADPKD and pathways that are modulated by curcumin and the ongoing developments regarding curcumin analogs and compounds with similar modes of action prompted us to investigate whether this multitarget drug might have therapeutic potential in the iKsp-$Pkd1^{del}$ model.

MATERIALS AND METHODS

Mice. Tamoxifen was administered orally at PN *days 40–42* to inducible kidney-specific *Pkd1*-deletion mice (tam-KspCad-CreERT2;$Pkd1^{lox2-11;lox2-11}$ or in short iKsp-$Pkd1^{del}$) as described previously (29, 30). Curcumin (~70% purity) was obtained from Sigma (Zwijndrecht, The Netherlands) and RM3(P) pellets with 1% curcumin or without curcumin were prepared by Special Diets Services (Witham, UK). This dose and way of administration were chosen in analogy to a recent experimental study that studied the effectiveness of curcumin to inhibit prostate carcinoma (3). Blood sampling and blood urea (BU) measurements were performed as described previously (18). Local animal experimental committee of the Leiden University Medical Center and the Commission Biotechnology in Animals of the Dutch Ministry of Agriculture approved the experiments performed.

Immunohistochemistry. After removal, kidneys were fixed O/N in buffered 4% formaldehyde solution and embedded in paraffin. Kidney sections (4 μm) were stained with standard hematoxylin and eosin or Periodic acid-Schiff (PAS). For immunohistochemical analysis, sections were deparaffinized and subjected to heat-mediated antigen retrieval [1 mM EDTA, pH 8.0 for anti-phospho-Stat3 (Tyr705) and 0.01 M citrate buffer, pH 6.0 for anti-phospho-ribosomal protein S6 (Ser240/244); Cell Signaling, no. 9145 and no. 2215S, respectively]. Sections were blocked with 0.1% H_2O_2 for 20 min for endogenous peroxidase activity and preincubated for 1 h with 5% normal goat serum in 1% BSA in PBS. Next, the sections were incubated O/N with anti-pSTAT3 (1:75), anti-p-rpS6 (1:100), rabbit anti-Ki-67 (1:3,000; Nova Castra), rabbit anti-megalin (1:500; Pathology LUMC, Leiden, the Netherlands) (11), goat anti-Tamm Horsfall protein (uromodulin, 1:500; Organon Teknika-Cappel, Turnhout, Belgium), or rabbit anti-aquaporin-2 (1:4,000; Calbiochem, Amsterdam, The Netherlands) in 1% BSA in PBS. Following incubation with rabbit envision horseradish peroxidase (HRP; DakoCytomation, Glostrup, Denmark) or rabbit-anti-goat HRP (1:300, Dako), immune reactions were revealed using diaminobenzidine as a chromogen and counterstained with hematoxylin, dehydrated, and mounted.

Cystic and proliferation index. For each mouse, the percentage of cystic area relative to total tissue was determined by Image J software (public domain software, National Institutes of Health) on 10 ×400 magnified photographs throughout the cortex on kidney sections stained with PAS. For the proliferation index, sections were stained for Ki-67 to visualize dividing cells. At least a thousand nuclei were counted per mouse and the proliferation index was calculated as the percentage of Ki-67-positive nuclei.

Cell culture and characterization. SV40 large T-antigen immortalized murine renal epithelial cells, derived from a $Pkd1^{lox,lox}$ mouse, were cultured in DMEM/F12 with glutamine and 15 mM HEPES, 100 U penicillin/streptomycin (Invitrogen, Breda, The Netherlands) supplemented with 2% Ultroser G (Pall BioSepra, Cergy, France), 2.5 μg/l prostaglandin E_1, 5 mg/l insulin-transferrin-sodium selenite, and 30 μg/l hydrocortisone obtained from Sigma. To obtain $Pkd1^{del,del}$ cells, $Pkd1^{lox,lox}$ cells were transfected with a Cre plasmid containing a neomycin resistance cassette using Lipofectamin 2000 Transfection Reagent (Invitrogen) according to the manufacturer's protocol. After transfection, the cells were cultured in selection medium [similar to medium described above but with 400 μg/ml geneticin (Invitrogen)] and diluted to obtain single clones that were tested for the *Pkd1* deletion by PCR (detailed information about the Cre construct and primer sequences can be provided by the corresponding author).

RNA and cDNA were obtained using Tri-Reagent (Sigma) and the Transcriptor First Strand cDNA Synthesis Kit (Roche, Almere, The Netherlands) according to the manufacturer's protocol. PCR was performed using primers for the proximal tubule marker Cubilin (Cubn) and for the collecting duct marker arginine vasopressin receptor 2 (Avpr2) and analyzed on a 2.5% agarose gel. Immunofluorescence using antibodies against β-catenin (1:100; BD Biosciences, Breda, The Netherlands) or α-tubulin (1:200; Sigma) was performed as described previously (29).

At 50% confluence, cells were incubated O/N with 0, 2.5, 5, or 10 μM curcumin (Sigma) in the absence of medium supplements. Then, the cells were incubated with the same curcumin concentrations in the presence of medium supplements for an additional 6 h. Protein lysates were prepared and analyzed by Western blot analysis as described below.

Western blot and densitometric analysis. Throughout the lysis procedure, 2 mM NaF, 1 mM Na_2VO_4, and protease inhibitor cocktail (Roche) were used to inhibit phosphatase and protease activity. Kidneys were homogenized in 600 μl RIPA without detergents (50 mM Tris·HCl, pH 7.4, 150 mM NaCl, 1 mM EDTA) using Magnalyser technology (Roche) followed by three 5-s pulses of sonication. Next, an equal amount of RIPA with detergents (50 mM Tris·HCl, pH 7.4, 150 mM NaCl, 1 mM EDTA, 2% DOC, 2% NP-40, 2% Triton X-100) was added and samples were incubated for 45 min at 4°C. Kidney lysates were spun-down for 10 min at 14,000 *g* and supernatants were stored at −80°C. Cell lysates were prepared by scraping the cells (50–80% confluent) from six-well dishes in 100 μl RIPA without detergents followed by three 5-s pulses of sonication. The rest of the procedure was similar to the kidney lysate preparation. Protein concentrations were determined using BCA protein assay (Thermo Fisher Scientific, Etten-Leur, The Netherlands). Ten micrograms of cell lysates and 80–120 μg of kidney lysates were used for SDS-PAGE and immunoblotting. Membranes were blocked for 1 h in 25% sea block blocking buffer (Thermo Fisher Scientific/Pierce, no. 37527, Etten-Leur, The Netherlands) in PBS and incubated O/N with anti-pSTAT3 (1:1,000), anti-STAT3 (Tyr705; 1:1,000; Cell Signaling, no. 9139), anti-p-rpS6(1:2,000), anti-rpS6 (Ser240/244; 1:1,000; Cell Signaling, no. 2317), or anti-β-actin (1:5,000; Cell Signaling, no. 4967) in 5% BSA-TBS (Tween 20, 0.1%). Goat-anti-rabbit (1:10,000) DyLight 800 (Perbio Science, no.35571) was used as secondary antibody for the detection of anti-pSTAT3, anti-p-rpS6, and anti-β-actin. Goat-anti-mouse DyLight 680 (1:10,000; Perbio Science, no. 35518) was used as secondary antibody for the detection of anti-STAT3 and anti-rpS6. Detection and densitometric analysis were carried out with the Odyssey Infrared Imaging System (Westburg, Leusden, The Netherlands). After detection, the same membrane was used to detect the next protein; i.e., after pSTAT3 detection, the same membrane was used to detect total STAT3 and then β-actin. Because total STAT3 and total rpS6 were detected with mouse antibodies (detected at 680 nm) and pSTAT3 and p-rpS6 with rabbit antibodies (detected at 800 nm), the total pool of protein could be easily discriminated from the phosphorylated variant. pSTAT3 nicely overlapped with total STAT3 and p-rpS6 overlapped with total rpS6. From each blot, protein levels were quantified using pSTAT3/STAT3 and p-rpS6/rpS6 integrated intensity ratios. β-Actin was used as a loading control.

Statistical analysis. Differences in Western blot/densitometric analysis of p-rpS6/rpS6 and pSTAT3/STAT3 ratios between cystic and control samples were tested by Student's *t*-tests. Differences in two-kidney weight/body weight (2KW/BW%) ratios, cystic and proliferation indexes, and Western blot/densitometric analysis of p-rpS6/rpS6 and pSTAT3/STAT3 ratios between untreated and curcumin-treated mice at the 11-wk time point were tested using Mann-Whitney *U*-tests. The Kaplan-Meier method was used to analyze overall survival of curcumin-treated and -untreated mice that were followed until the onset of renal failure and the significance of differences between those groups was analyzed by the Log-Rank (Mantel-Cox) test adjusted for litter effects.

RESULTS

Curcumin and PKD-related pathways. The ability of curcumin to inhibit mTOR and Wnt signaling is likely to be relevant for ADPKD since these signaling routes are altered during cystogenesis (4, 5, 18, 23, 27, 32, 55). Previously, we and others showed that cystogenesis is accompanied by up-regulation of several canonical Wnt targets, including cyclin D1 and survivin (18, 27). Since these genes are also direct targets of STAT3, a transcription factor that is frequently activated in several types of tumors, we investigated possible STAT3 activation in iKsp-*Pkd1*[del] mice (8, 17, 33, 49, 50, 52). In these mice, *Pkd1* inactivation by tamoxifen treatment at *days 40–42* results in end-stage PKD ~16 wk later (Fig. 1*B*). Immunohistochemical analysis of renal sections demonstrated numerous regions with strong nuclear accumulation of phosphorylated-(Tyr705)-STAT3 (pSTAT3) in cyst-lining epithelial cells and in interstitial cells, while in kidneys of control mice only few pSTAT3-positive nuclei were observed (Fig. 1, *C* and *D*). To further quantify STAT3 activity, total and phosphorylated STAT3 levels were analyzed by Western blot and densitometric analysis. Whereas total STAT3 increased slightly, which did not reach statistical significance, the pSTAT3/STAT3 ratio was strongly elevated in cystic mice and thus revealed that STAT3 was strongly activated in cystic kidneys, thereby confirming the immunohistological data ($P <$ 0.01; Fig. 2, *A* and *C*).

The relevance of mTOR signaling in ADPKD has previously been demonstrated in a number of ADPKD models where inhibition of mTOR by rapamycin resulted in reduced cyst progression (55, 56, 61). To confirm mTOR activation, ribosomal protein S6 (rpS6) that acts downstream from the mTOR/S6K pathway was analyzed. Numerous cysts displayed intense p-rpS6 levels in cyst-lining epithelial cells, whereas in control mice only negative and weak-to-moderate p-rpS6 expression could be observed (Fig. 1, *E* and *F*). Also, Western blot analysis indicated strong activation of rpS6 in cystic kidneys, whereas total levels were not different ($P <$ 0.01; Fig. 2, *B* and *D*). Sequential sections stained with antibodies against pSTAT3, p-rpS6, and markers for proximal tubules (megalin), distal tubules (Tamm-Horsfall protein), and collecting ducts (aquaporin-2) revealed that STAT3 and rpS6 activation occurred in all tubular segments (Fig. 1, *G–M*). These data suggest that mTOR but also STAT3 is activated in PKD.

Interestingly, activation of these proteins is known to be inhibited by curcumin (4, 5, 10, 26). To confirm the effect of curcumin on STAT3 and mTOR activation, we performed in vitro experiments on immortalized renal tubular epithelial cells that were derived from *Pkd1*[lox,lox] mice. These cells likely

originate from the proximal epithelium since they express the proximal marker Cubn but not the collecting duct marker Avpr2 (Supplementary Fig. S1*C*; the online version of this article contains supplemental data). They were also able to form cilia, as detected by α-tubulin, and expressed β-catenin in the plasma membrane (Supplementary Fig. S1, *A* and *B*). A subclone was transfected with a Cre plasmid to generate *Pkd1*[del,del] cells and a pcr was performed to confirm the deletion (Supplementary Fig. S1*D*). Both *Pkd1*[lox,lox] and *Pkd1*[del,del] cells were incubated with different curcumin concentrations (0, 2.5, 5, and 10 μM) and analyzed for pSTAT3/STAT3 and p-rpS6/rpS6 ratios. β-Actin was used as a loading control. Both cell lines demonstrated a comparable dose-dependent reduction of STAT3 and rpS6 activation, indicating that curcumin inhibits both pathways regardless of *Pkd1* expression (Fig. 3, *A–D*).

Curcumin inhibits cystogenesis in vivo. Given the apparent overlap between curcumin-targeted and PKD-related pathways, we set out to investigate the therapeutic potential of curcumin in our previously developed iKsp-*Pkd1*[del] mouse model (29, 30). An overview of the treatment strategy is given in Fig. 4 and was performed as follows: at PN *days 40–42*, we administered tamoxifen to male iKsp-*Pkd1*[del] mice to inactivate *Pkd1*. Seven days after gene disruption, each litter was divided into a control and a curcumin group. Control mice were put on a standard diet and curcumin mice received the same diet supplemented with 1% curcumin. The mice were followed in time and killed after ascertainment of renal failure where a BU concentration of 20 mmol/l or higher was used as criterion (long-treatment group). In addition, a subgroup of mice was killed 11 wk after gene disruption (short-treatment group). For both groups, there was no difference in total body weight between curcumin-treated and -untreated mice (Supplementary Fig. S2*A*). Control mice that did not receive tamoxifen had normal kidneys (Fig. 1*A*). Mice that did receive tamoxifen and killed 11 wk later ($n = 5$ from 2 litters) displayed tubular dilations and small cysts accompanied by increased 2KW/BW% (median 2.6%), cystic index (CI; median 44%), and proliferation index (PI; median 4.2%; Figs. 5*A* and 6). These parameters were significantly reduced in curcumin-treated littermates ($n = 5$; 2KW/BW% = 1.9%, $P <$ 0.01; CI = 34%, $P <$ 0.05; and PI = 3%, $P <$ 0.01), which also corresponded to improved histology (Figs. 5, *A* and *B*, and 6). To assess whether besides proliferation also apoptosis took part in the curcumin-mediated reduction in cystogenesis, we stained kidney sections from curcumin-treated and -untreated mice for cleaved caspase-3 but found only very few apoptotic cells, indicating that apoptosis did not play a significant role (data not shown).

From mice that were followed until the onset of renal failure (long treatment), BU was measured on a weekly basis. When BU exceeded 15 mmol/l, the frequency of the measurements was increased to pinpoint the moment of renal failure. Both curcumin-treated and -untreated mice reached renal failure. However, curcumin treatment postponed renal failure in all five litters tested (Fig. 7*A*; also shown combined in Supplementary Fig. S2*B*). The median survival after tamoxifen treatment for all curcumin-treated mice ($n = 12$) was 119 days and for all untreated mice ($n = 11$) 105 days. Kaplan-Meier analysis showed that both groups significantly differed from each other ($P <$ 0.001; Fig. 7*B*). Taken together, these data
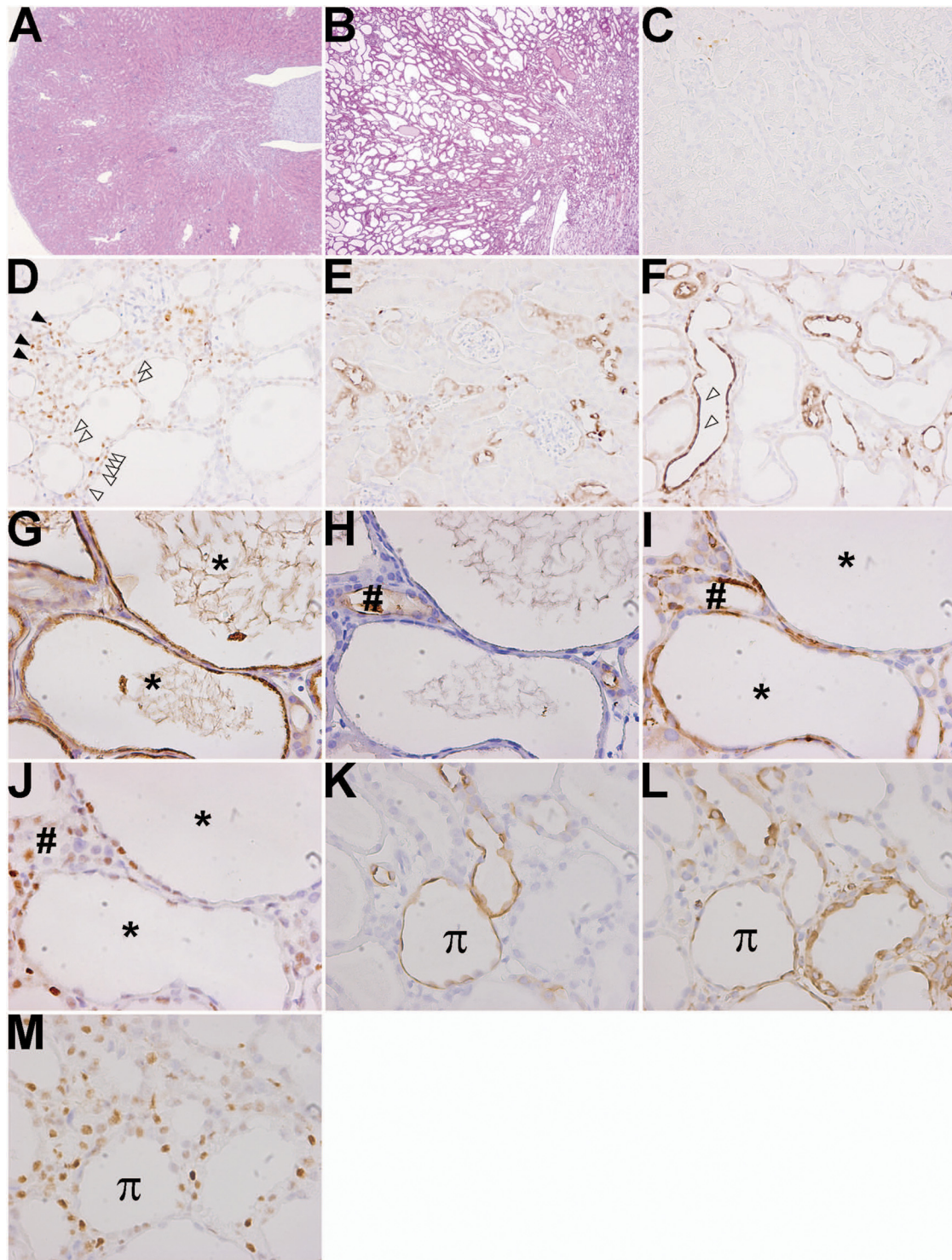
Fig. 1. Expression of phosphorylated signal transducers and activator of transcription 3 (STAT3) and ribosomal protein S6 (rpS6) in cystic kidneys from iKsp-*Pkd1*[del] mice. *A–F*: iKsp-*Pkd1*[del] mice untreated (*A*, *C*, and *E*) or treated (*B*, *D*, and *F–M*) with tamoxifen and killed ~16 wk later (for mice that received tamoxifen, this means that they developed renal failure). *A* and *B*: hematoxylin and eosin (HE) staining indicating normal histology in mice without tamoxifen treatment and severe cystic disease 4 mo after tamoxifen administration. *C* and *D*: phosphorylated-(Tyr705)-STAT3 (pSTAT3) staining could hardly be observed in control mice but regions with intense staining were observed in mice with polycystic kidney disease (PKD; examples of positive cystic epithelial and interstitial nuclei are indicated by open and closed arrowheads, respectively). *E* and *F*: mosaic staining pattern for phosphorylated-rpS6 (p-rpS6) in control and cystic mice showing more areas with increased intensity in cystic kidneys; indicated by arrowheads. *G–J*: sequential sections of a cystic area stained for the proximal marker megalin (*G*), the distal marker Tamm-Horsfall protein (*H*), p-rpS6 (*I*), and pSTAT3 (*J*). Overlap between megalin, pSTAT3, and p-rpS6 is indicated by * and overlap between Tamm-Horsfall protein, pSTAT3, and p-rpS6 by #. *K–M*: sequential sections of a cystic area stained for the collecting duct marker aquaporin-2 (*K*), p-rpS6 (*L*), and pSTAT3 (*M*). Overlap between aquaporin-2, pSTAT3, and p-rpS6 is indicated by π. Magnifications were ×25 for *A* and *B*, ×200 for *C–F*, and ×400 for *G–M*.
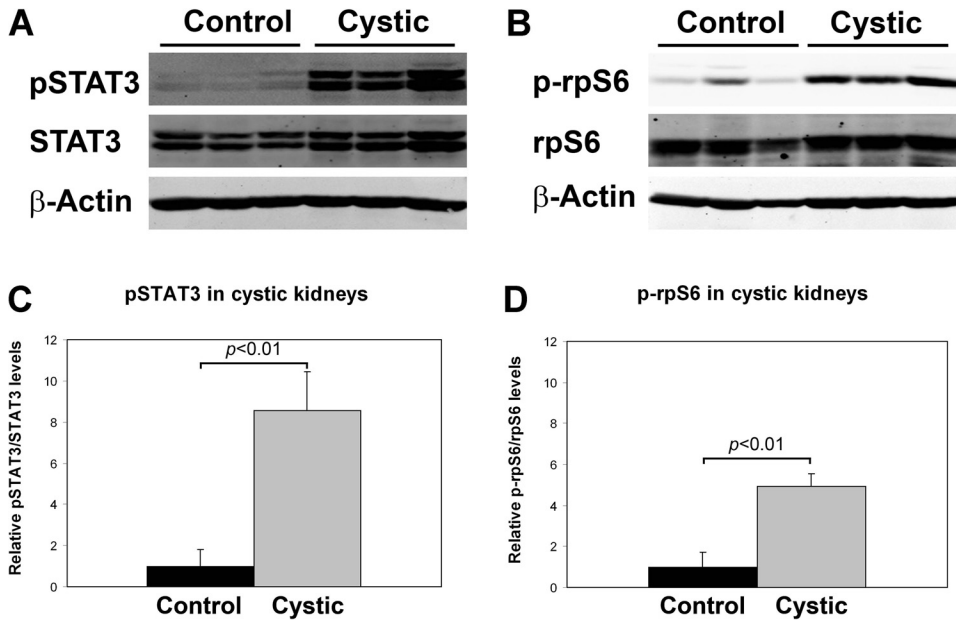
Fig. 2. Activation of STAT3 and rpS6 in PKD. *A* and *B*: total kidney lysates from iKsp-*Pkd1*[del] mice with end-stage PKD (cystic) or control mice that did not receive tamoxifen (control) were immunoblotted and incubated with an antibody against pSTAT3 and STAT3 (*A*; detecting both pSTAT3α and β) or against p-rpS6 and rpS6 (*B*). β-Actin was used as loading control. pSTAT3 can hardly be detected in controls, whereas cystic samples show strong pSTAT3 expression. Total STAT3 levels only slightly increased in cystic mice (not significant). Also, p-rpS6 levels are increased in cystic kidneys, whereas total levels were not different. Densitometric analysis reveals significant differences in pSTAT3/STAT3 (*C*) and p-rpS6/rpS6 (*D*) ratios ($P < 0.01$, Student's *t*-test). Error bars indicate standard deviations.

demonstrate that curcumin treatment reduces proliferation resulting in inhibited cystogenesis and delayed renal failure.

Involvement of pSTAT3 and p-rpS6. To investigate whether STAT3 and mTOR signaling contributed to the curcumin-mediated inhibition of cystogenesis, we performed immunohistochemical and Western blot analysis on the short-treatment group.

Immunohistochemical staining of pSTAT3 revealed that the reduction of the cystic phenotype by curcumin treatment correlated with fewer nuclei expressing active STAT3 (Fig. 5, *C* and *D*). Also, Western blot analysis on the short-treatment groups showed clear activation of STAT3 in untreated mice that was significantly reduced in curcumin-treated mice ($P < 0.01$; Fig. 8, *A* and *C*). In kidneys from untreated and cur-

cumin-treated mice that had been followed until renal failure (long treatment), pSTAT3 levels did not differ but were higher compared with the short-treatment group (Supplementary Fig. S3, *A* and *C*).

Also, rpS6 was analyzed in the short-treatment group. Although expression of p-rpS6 appeared slightly reduced in curcumin-treated mice (Fig. 5, *E* and *F*), the reduction observed by Western blotting did not reach statistical significance (Fig. 8, *B* and *D*). Also, the activation of rpS6 compared with controls was not significant, indicating that the role of mTOR at this stage of the disease is limited. RpS6 was clearly activated in the long-treatment groups and curcumin-treated mice displayed a similar reduced yet statistically insignificant trend (Supplementary Fig. S3, *B* and *D*).
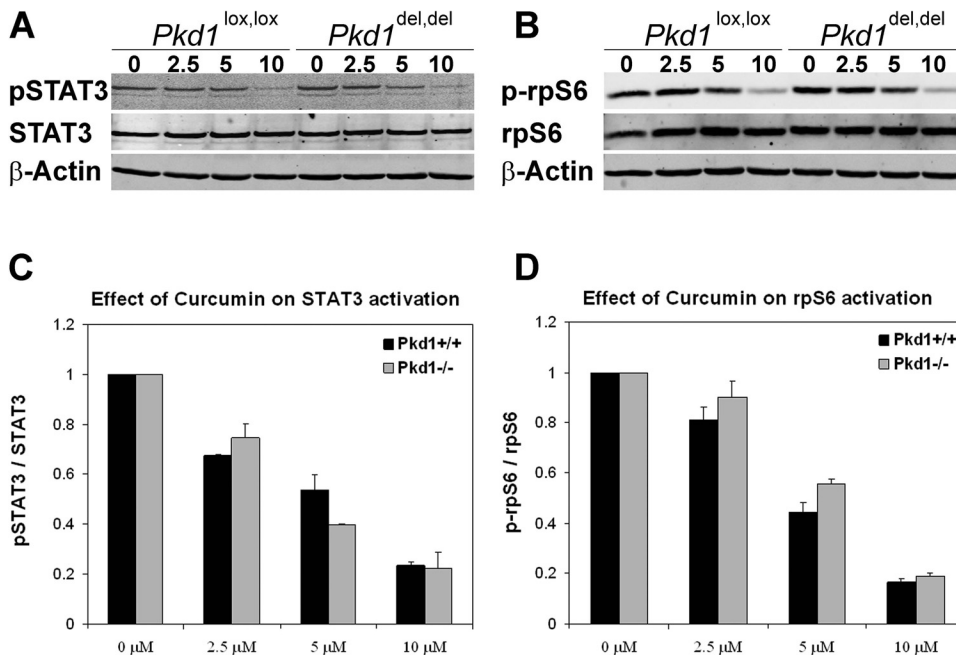

Fig. 3. In vitro effect of curcumin on STAT3 and rpS6 activation. *Pkd1*[lox,lox] and *Pkd1*[del,del] cells were cultured in the presence of 0, 2.5, 5, or 10 μM curcumin. In both cell lines, Western blot analysis demonstrates a dose-dependent reduction of pSTAT3 levels relative to total STAT3 (*A* and *C*). Also, p-rpS6/rpS6 ratios were reduced on increasing curcumin concentrations (*B* and *D*).
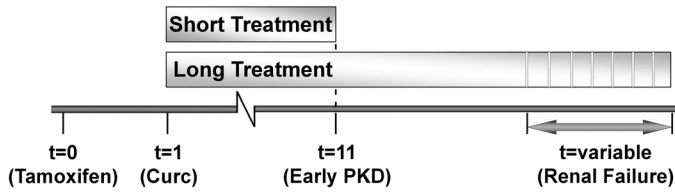
Fig. 4. In vivo experimental setup. Tamoxifen is administered to iKsp-*Pkd1*^{del} mice at postnatal (PN) *days 40–42* (*t* = 0) to induce conversion of the *Pkd1*^{lox} to the inactive *Pkd1*^{del} allele. One week later, mice either continued to receive normal food or food supplemented with 1% curcumin. One group was killed 11 wk after tamoxifen (short treatment). Another group was followed until renal failure [blood urea (BU) > 20 mmol/l], meaning that in this group, the time at which mice are killed is the read-out (long treatment).

These data indicate that STAT3 is already activated at a relatively early stage of PKD and suggest that the curcumin-mediated inhibition of cyst formation at least in part acts through STAT3 inhibition. However, mTOR was only significantly activated at end-stage PKD and although curcumin treatment resulted in reduced activation in both the short- and long-treatment groups, this effect was not significant.

DISCUSSION

In ADPKD, cyst development is preceded by a critical cellular drop in PC1 and/or PC2 levels resulting in deregulation of many signaling pathways that control proliferation, differentiation, PCP, cell-cell and cell/matrix communication, and fluid transport (13, 43, 44, 67). Altered expression of PCP-related genes such as *Fjx1* and *Fat4* has been linked to cystogenesis possibly by causing disturbed centrosome positioning of newly formed cells after cell division (18, 51). We observed downregulation of *Fjx1* in *Pkd1*-deletion mice during tissue repair when normally its expression is required (18). This apparent defect in PCP signaling, which is regulated by noncanonical Wnt signaling, was accompanied by increased expression of canonical Wnt targets (18). Moreover, their expression has also been demonstrated to be elevated in human cystic samples (27). Together with the ability of the COOH-terminal tail of PC1 to physically interact with and thereby suppress the activity of β-catenin, these data suggest important links between Wnt signaling and cystogenesis (27).

Expression of canonical Wnt targets, however, may not be exclusively accountable to Wnt signaling. For example, cyclin D1 and survivin are also known targets of STAT3, a transcription factor that, when activated in several types of tumors, is associated with poor prognosis (8, 17, 33, 50, 52). Although STAT3 promotes cell survival and proliferation, it has been demonstrated that overexpression of *PKD1* in vitro could activate a STAT3 luciferase reporter construct (7, 49). In-
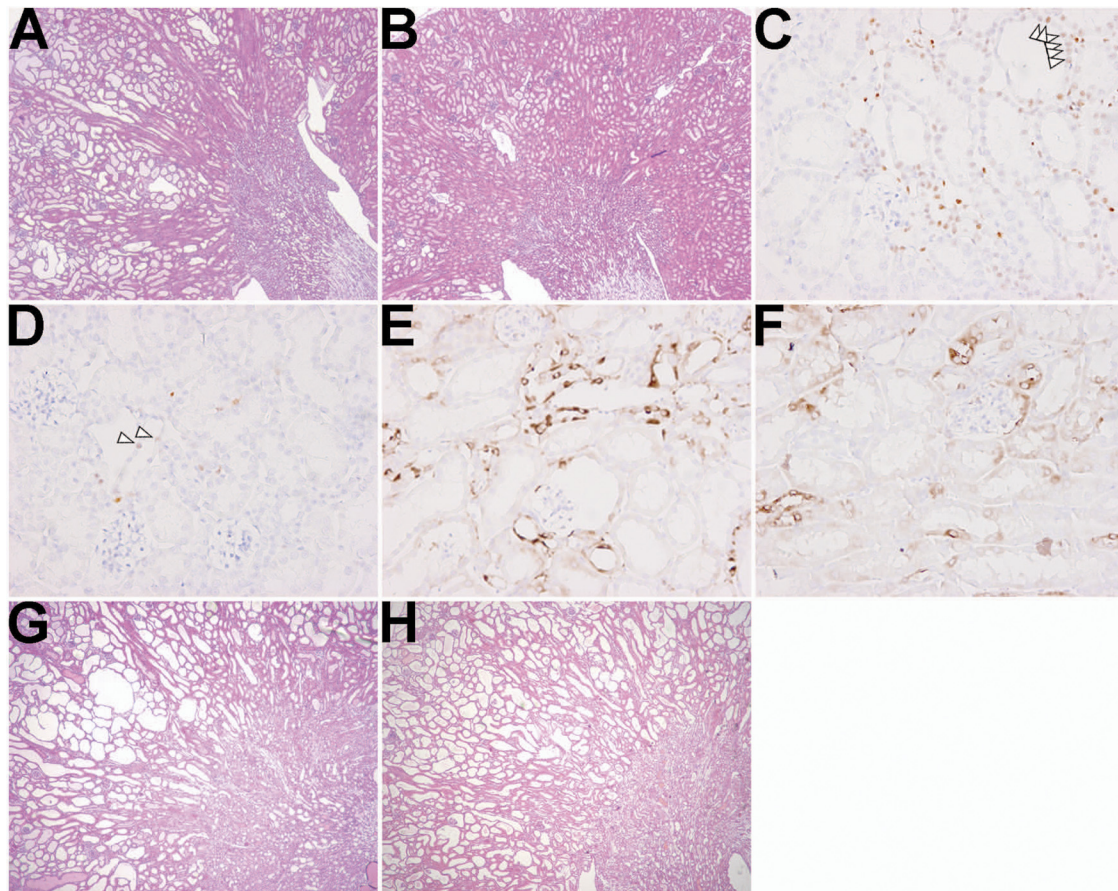

Fig. 5. Effect of curcumin treatment on iKsp-*Pkd1*^{del} mice. *A–F*: most severely affected iKsp-*Pkd1*^{del} mice in the short-treatment group without (*A, C,* and *E*) or with (*B, D,* and *F*) curcumin treatment. After curcumin treatment, HE staining indicated improved histology (*A* and *B*), decreased nuclear pSTAT3 staining (*C* and *D*), and to a lesser extent decreased p-rpS6 staining (*E* and *F*); arrowheads indicate examples of positive pSTAT3 nuclei. Both untreated (*G*; 93 days after tamoxifen) and curcumin-treated (*H*; 117 days after tamoxifen) reached renal failure as a consequence of severe PKD. Magnifications were ×25 for HE stainings and ×200 for pSTAT3 and p-rpS6 stainings.
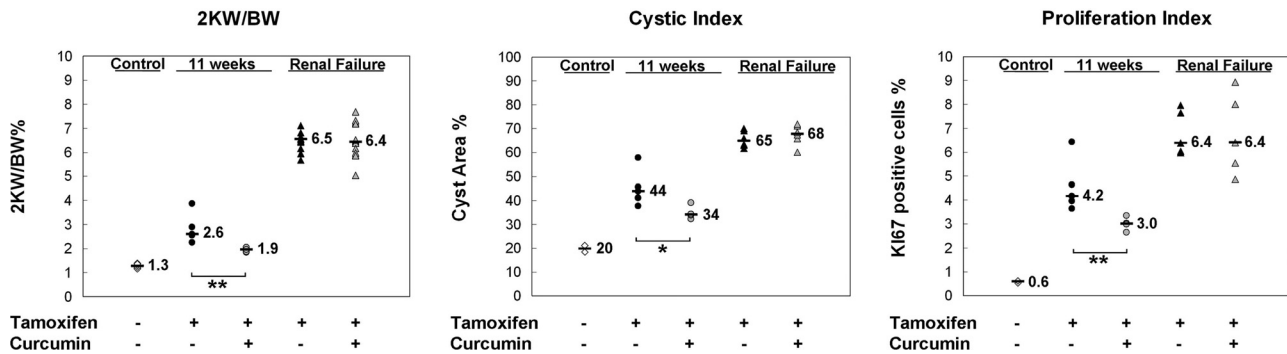
Fig. 6. Effect of curcumin treatment on 2-kidney weight/body weight (2KW/BW) ratios, cystic and proliferation indexes. Curcumin-treated iKsp-*Pkd1*[del] mice that were killed 11 wk after *Pkd1* disruption showed significant lower 2KW/BW ratios (1.9%) compared with their untreated littermates (2.6%; $P < 0.01$). In line with the 2KW/BW ratios, the cystic area and the number of proliferating cells, as determined by Ki-67 staining, were lower in the curcumin-treated mice (44 vs. 34%, $P < 0.05$ and 4.2 vs. 3.0%, $P < 0.01$, respectively). These parameters increased in mice that were followed until renal failure but there was no difference between untreated and curcumin-treated mice other than the time frame within renal failure developed.

creased phosphorylation levels, however, were not detected (7). In the same study, the closely linked but counteracting STAT1 was analyzed. Overexpression of *PKD1* in Madin-Darby canine kidney (MDCK) cells resulted in enhanced STAT1 activation and subsequent p21[waf]-induced G0/G1 growth arrest. In line with these results, *Pkd1*^{−/−} embryos indeed exhibited reduced pSTAT1 and p21[waf1] levels (7). Although the exact contribution remains to be elucidated, our observations indicate that STAT3 activation strongly correlates with increased cyst progression.
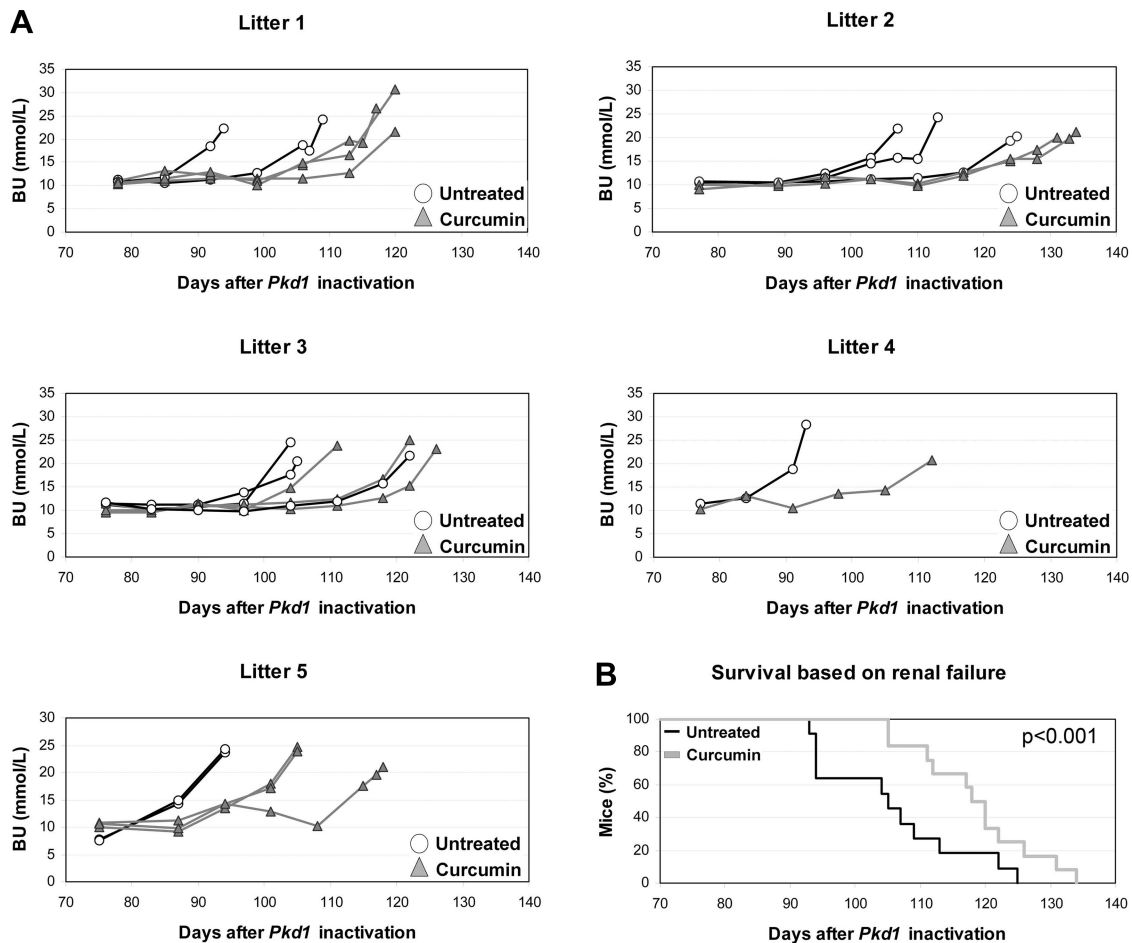

Fig. 7. Curcumin treatment delays renal failure in iKsp-*Pkd1*[del] mice in the long-treatment groups. *A*: from 11 wk after *Pkd1* disruption, BU was measured on a weekly basis in curcumin-treated and -untreated iKsp-*Pkd1*[del] mice until renal failure (BU > 20 mmol/l) was ascertained. Curcumin treatment delayed renal failure in all 5 litters tested. *B*: Kaplan-Meier analysis of all litters combined revealed a significant difference between the untreated and curcumin-treated mice ($P < 0.001$, Log-Rank test adjusted for litter). The median survival of untreated mice ($n = 11$) was 105 days and of curcumin-treated mice ($n = 12$) 119 days after *Pkd1* disruption.
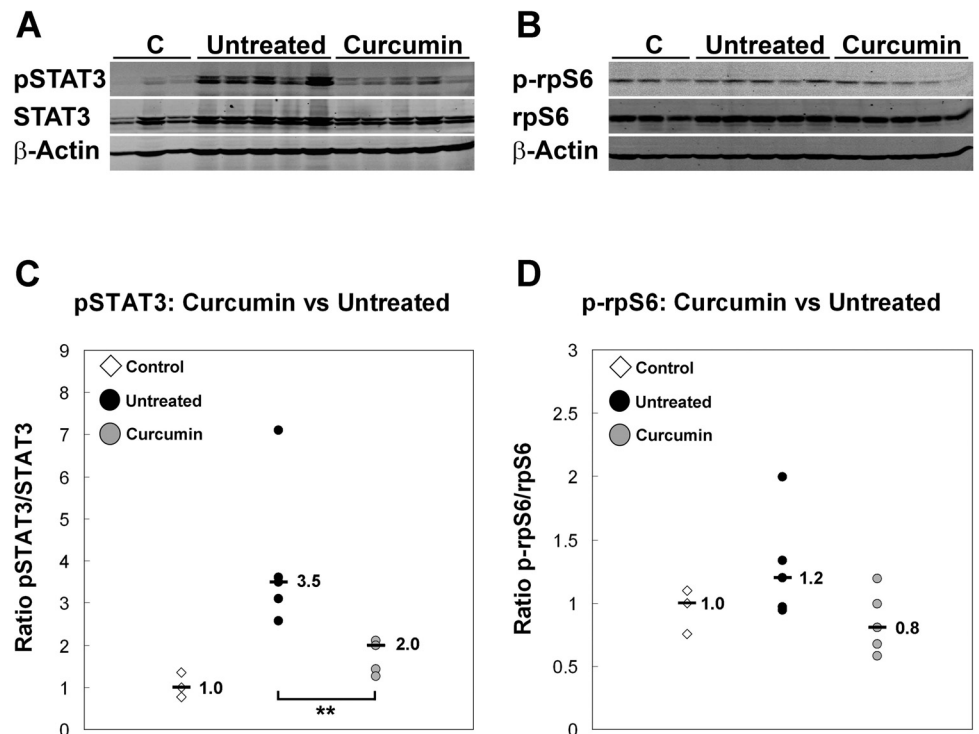
Fig. 8. Expression of pSTAT3 and p-rpS6 in curcumin-treated and -untreated iKsp-$Pkd1^{del}$ mice in the short-treatment groups. Representative Western blot analysis on protein extracts from control mice (c) and curcumin-treated and -untreated iKsp-$Pkd1^{del}$ mice that were killed 11 wk after $Pkd1$ disruption to determine pSTAT3/STAT3 (*A*) or p-rpS6/rpS6 ratios (*B*). β-Actin was used as a loading control. *C*: STAT3 is activated 11 wk after $Pkd1$ disruption and curcumin treatment reduces STAT3 activation ($P <$ 0.01). *D*: at this stage of the disease, there was no significant elevation in p-rpS6 compared with wild-type mice. The reduction of p-rpS6 in curcumin-treated mice did not reach statistical significance.

Another crucial modulator of proliferation that is activated in ADPKD is mTOR. It has been shown that, together with tuberin, the COOH-terminal tail of PC1 forms a complex with mTOR, thereby reducing its activity (55). The ability of mTOR inhibitors to greatly reduce cystogenesis in several animal models further supports its role in ADPKD (55, 56, 61). However, the promising results in rodents seem to contrast the data obtained in recent clinical trials that at best demonstrate mild benefits (45, 53, 66). We observed a dose-dependent effect of an mTOR inhibitor on mTOR signaling and on renal cystic disease in our iKsp-$Pkd1^{del}$ mice (Novalic Z, unpublished data). Of note, it has also been shown that the serum concentration of mTOR inhibitors that can be used in clinical practice is too low to inhibit tissue mTOR (9). The results obtained in clinical trials in ADPKD patients with mTOR inhibitors do therefore not preclude a role for mTOR activation. To study whether mTOR may be involved in iKsp-$Pkd1^{del}$ mice, we analyzed activation of rpS6, a downstream target of the mTOR/S6K pathway, and indeed observed increased phosphorylation of rpS6 in cystic kidneys.

Altered regulation of these and other signaling pathways, likely to be subject to extensive cross talk, ultimately results in cyst formation. Given these complex networks of altered signaling in ADPKD, we reasoned that compounds targeting a variety of these routes, as opposed to compounds specifically acting on a single target, may provide new therapeutic insights. Curcumin has been shown to be safe and effective in treating several inflammatory and malignant diseases, mostly in rodent models, by modulating a wide range of pathways that are also altered in ADPKD (3–5, 10, 16, 22, 23, 27, 31, 32, 35, 55, 56, 59, 61, 69). In addition, during the preparation of this manuscript, it has been demonstrated that curcumin retards cyst development in MDCK cysts grown in collagen gels and in cultured embryonic kidneys (15).

We demonstrate here that curcumin indeed causes a dose-dependent reduction in rpS6 and STAT3 activation in $Pkd1^{lox,lox}$ and

$Pkd1^{del,del}$ cells and that cystogenesis is inhibited in iKsp-$Pkd1^{del}$ mice. Eleven weeks after $Pkd1$ disruption, an approximate twofold increase in 2KW/BW ratio was observed accompanied by mild to severe tubular dilatations mostly in the cortical region of the kidney. Curcumin treatment significantly reduced cystic and proliferation indexes, 2KW/BW ratios, and improved renal histology. In line with these results, the onset of renal failure in mice that were followed further in time was significantly postponed. Although the exact mechanism likely comprises additional pathways, the correlation between the improved renal phenotype by curcumin treatment and reduced STAT3 signaling supports the involvement of STAT3.

Levels of p-rpS6 were not yet significantly elevated in untreated mice at the 11-wk time point. The small and statistically insignificant effect of curcumin on mTOR signaling at this stage is therefore not a major contributor for the reduced cystic phenotype in these mice. However, we cannot exclude an effect on mTOR signaling at more advanced stages of the disease.

Curcumin was not able to prevent cystogenesis entirely, which may be a consequence of its limited bioavailability. Many studies addressed this issue, leading to curcumin analogs with improved pharmacological profiles and new delivery methods for curcumin (1, 21, 25, 36, 40, 57). In addition, the generation of a series of synthetic derivatives of oleanolic acid, a triterpenoid that can be found in olives, may be an interesting candidate for ADPKD treatment (20, 39). These synthetic oleanane triterpenoids (SO) act on similar pathways as curcumin possibly by the so-called Michael acceptor properties that both these molecules possess (39). One such SO, CDDO-Me, seems to be active at lower concentrations than curcumin, has successfully been tested in rodent models against several malignant diseases, and is currently being tested in phase I and phase II clinical trials (37–39, 47). An additional property of curcumin-like molecules and SO that was not tested in this study but may be of relevance to ADPKD is their ability to reduce kidney damage by acting as antioxidants and by

inducing a series of cytoprotective genes through Nrf2 activation (2, 16, 22). Since we and others showed that cyst progression is greatly accelerated by these kind of stress factors, it would be interesting to see whether alleviating kidney damage by this strategy could slow down the observed acceleration in cyst progression (18, 60).

In conclusion, this study provides evidence that multitarget compounds like curcumin are able to inhibit cyst progression without apparent side effects. Current developments in the field of curcumin analogs and SO are highly promising and should be further evaluated as possible therapeutics for ADPKD.

REFERENCES

1. **Amolins MW, Peterson LB, Blagg BS.** Synthesis and evaluation of electron-rich curcumin analogs. *Bioorg Med Chem* 17: 360–367, 2009.
2. **Balogun E, Hoque M, Gong P, Killeen E, Green CJ, Foresti R, Alam J, Motterlini R.** Curcumin activates the haem oxygenase-1 gene via regulation of Nrf2 and the antioxidant-responsive element. *Biochem J* 371: 887–895, 2003.
3. **Barve A, Khor TO, Hao X, Keum YS, Yang CS, Reddy B, Kong AN.** Murine prostate cancer inhibition by dietary phytochemicals–curcumin and phenyethylisothiocyanate. *Pharm Res* 25: 2181–2189, 2008.
4. **Beevers CS, Chen L, Liu L, Luo Y, Webster NJ, Huang S.** Curcumin disrupts the Mammalian target of rapamycin-raptor complex. *Cancer Res* 69: 1000–1008, 2009.
5. **Beevers CS, Li F, Liu L, Huang S.** Curcumin inhibits the mammalian target of rapamycin-mediated signaling pathways in cancer cells. *Int J Cancer* 119: 757–764, 2006.
6. **Belibi FA, Edelstein CL.** Novel targets for the treatment of autosomal dominant polycystic kidney disease. *Expert Opin Investig Drugs* 19: 315–328, 2010.
7. **Bhunia AK, Piontek K, Boletta A, Liu L, Qian F, Xu PN, Germino FJ, Germino GG.** PKD1 induces p21(waf1) and regulation of the cell cycle via direct activation of the JAK-STAT signaling pathway in a process requiring PKD2. *Cell* 109: 157–168, 2002.
8. **Bromberg JF, Wrzeszczynska MH, Devgan G, Zhao Y, Pestell RG, Albanese C, Darnell JE Jr.** Stat3 as an oncogene. *Cell* 98: 295–303, 1999.
9. **Canaud G, Knebelmann B, Harris PC, Vrtovsnik F, Correas JM, Pallet N, Heyer CM, Letavernier E, Bienaime F, Thervet E, Martinez F, Terzi F, Legendre C.** Therapeutic mTOR inhibition in autosomal dominant polycystic kidney disease: what is the appropriate serum level? *Am J Transplant* 10: 1701–1706, 2010.
10. **Chakravarti N, Myers JN, Aggarwal BB.** Targeting constitutive and interleukin-6-inducible signal transducers and activators of transcription 3 pathway in head and neck squamous cell carcinoma cells by curcumin (diferuloylmethane). *Int J Cancer* 119: 1268–1275, 2006.
11. **Christensen EI, Nielsen S, Moestrup SK, Borre C, Maunsbach AB, De Heer E, Ronco P, Hammond TG, Verroust P.** Segmental distribution of the endocytosis receptor gp330 in renal proximal tubules. *Eur J Cell Biol* 66: 349–364, 1995.
12. **Dhillon N, Aggarwal BB, Newman RA, Wolff RA, Kunnumakkara AB, Abbruzzese JL, Ng CS, Badmaev V, Kurzrock R.** Phase II trial of curcumin in patients with advanced pancreatic cancer. *Clin Cancer Res* 14: 4491–4499, 2008.
13. **Fischer E, Legue E, Doyen A, Nato F, Nicolas JF, Torres V, Yaniv M, Pontoglio M.** Defective planar cell polarity in polycystic kidney disease. *Nat Genet* 38: 21–23, 2006.
14. **Gabow PA.** Autosomal dominant polycystic kidney disease: more than a renal disease. *Am J Kidney Dis* 16: 403–413, 1990.
15. **Gao J, Zhou H, Lei T, Zhou L, Li W, Li X, Yang B.** Curcumin inhibits renal cyst formation and enlargement in vitro by regulating intracellular signaling pathways. *Eur J Pharmacol* 654: 92–99, 2011.
16. **Ghosh SS, Massey HD, Krieg R, Fazelbhoy ZA, Ghosh S, Sica DA, Fakhry I, Gehr TW.** Curcumin ameliorates renal failure in 5/6 nephrectomized rats: the role of inflammation. *Am J Physiol Renal Physiol* 296: F1146–F1157, 2009.
17. **Gritsko T, Williams A, Turkson J, Kaneko S, Bowman T, Huang M, Nam S, Eweis I, Diaz N, Sullivan D, Yoder S, Enkemann S, Eschrich S, Lee JH, Beam CA, Cheng J, Minton S, Muro-Cacho CA, Jove R.** Persistent activation of stat3 signaling induces survivin gene expression and confers resistance to apoptosis in human breast cancer cells. *Clin Cancer Res* 12: 11–19, 2006.
18. **Happe H, Leonhard WN, van der Wal A, van de Water B, Lantinga-van Leeuwen IS, Breuning MH, De Heer E, Peters DJ.** Toxic tubular injury in kidneys from Pkd1-deletion mice accelerates cystogenesis accompanied by dysregulated planar cell polarity and canonical Wnt signaling pathways. *Hum Mol Genet* 18: 2532–2542, 2009.
19. **Hogan MC, Masyuk TV, Page LJ, Kubly VJ, Bergstralh EJ, Li X, Kim B, King BF, Glockner J, Holmes DR III, Rossetti S, Harris PC, LaRusso NF, Torres VE.** Randomized clinical trial of long-acting somatostatin for autosomal dominant polycystic kidney and liver disease. *J Am Soc Nephrol* 21: 1052–1061, 2010.
20. **Honda T, Rounds BV, Bore L, Finlay HJ, Favaloro FG Jr, Suh N, Wang Y, Sporn MB, Gribble GW.** Synthetic oleanane and ursane triterpenoids with modified rings A and C: a series of highly active inhibitors of nitric oxide production in mouse macrophages. *J Med Chem* 43: 4233–4246, 2000.
21. **Huang MT, Lou YR, Xie JG, Ma W, Lu YP, Yen P, Zhu BT, Newmark H, Ho CT.** Effect of dietary curcumin and dibenzoylmethane on formation of 7,12-dimethylbenz[a]anthracene-induced mammary tumors and lymphomas/leukemias in Sencar mice. *Carcinogenesis* 19: 1697–1700, 1998.
22. **Iqbal M, Okazaki Y, Okada S.** Curcumin attenuates oxidative damage in animals treated with a renal carcinogen, ferric nitrilotriacetate (Fe-NTA): implications for cancer prevention. *Mol Cell Biochem* 324: 157–164, 2009.
23. **Jaiswal AS, Marlow BP, Gupta N, Narayan S.** Beta-catenin-mediated transactivation and cell-cell adhesion pathways are important in curcumin (diferuylmethane)-induced growth arrest and apoptosis in colon cancer cells. *Oncogene* 21: 8414–8427, 2002.
24. **Jurenka JS.** Anti-inflammatory properties of curcumin, a major constituent of Curcuma longa: a review of preclinical and clinical research. *Altern Med Rev* 14: 141–153, 2009.
25. **Khor TO, Yu S, Barve A, Hao X, Hong JL, Lin W, Foster B, Huang MT, Newmark HL, Kong AN.** Dietary feeding of dibenzoylmethane inhibits prostate cancer in transgenic adenocarcinoma of the mouse prostate model. *Cancer Res* 69: 7096–7102, 2009.
26. **Kunnumakkara AB, Anand P, Aggarwal BB.** Curcumin inhibits proliferation, invasion, angiogenesis and metastasis of different cancers through interaction with multiple cell signaling proteins. *Cancer Lett* 269: 199–225, 2008.
27. **Lal M, Song X, Pluznick JL, Di Giovanni V, Merrick DM, Rosenblum ND, Chauvet V, Gottardi CJ, Pei Y, Caplan MJ.** Polycystin-1 C-terminal tail associates with beta-catenin and inhibits canonical Wnt signaling. *Hum Mol Genet* 17: 3105–3117, 2008.
28. **Lantinga-van Leeuwen IS, Dauwerse JG, Baelde HJ, Leonhard WN, van der Wal A, Ward CJ, Verbeek S, Deruiter MC, Breuning MH, De Heer E, Peters DJ.** Lowering of Pkd1 expression is sufficient to cause polycystic kidney disease. *Hum Mol Genet* 13: 3069–3077, 2004.
29. **Lantinga-van Leeuwen IS, Leonhard WN, van der Wal A, Breuning MH, De Heer E, Peters DJM.** Transgenic mice expressing tamoxifen-inducible Cre for somatic gene modification in renal epithelial cells. *Genesis* 44: 225–232, 2006.
30. **Lantinga-van Leeuwen IS, Leonhard WN, van der Wal A, Breuning MH, De Heer E, Peters DJ.** Kidney-specific inactivation of the Pkd1 gene induces rapid cyst formation in developing kidneys and a slow onset of disease in adult mice. *Hum Mol Genet* 16: 3188–3196, 2007.
31. **Le N, van der Wal A, van der Bent P, Lantinga-van Leeuwen IS, Breuning MH, van Dam H, De Heer E, Peters DJ.** Increased activity of activator protein-1 transcription factor components ATF2, c-Jun, and c-Fos in human and mouse autosomal dominant polycystic kidney disease. *J Am Soc Nephrol* 16: 2724–2731, 2005.

32. **Leow PC, Tian Q, Ong ZY, Yang Z, Ee PL.** Antitumor activity of natural compounds, curcumin and PKF118–310, as Wnt/beta-catenin antagonists against human osteosarcoma cells. *Invest New Drugs* 28: 766–782, 2010.

33. **Leslie K, Lang C, Devgan G, Azare J, Berishaj M, Gerald W, Kim YB, Paz K, Darnell JE, Albanese C, Sakamaki T, Pestell R, Bromberg J.** Cyclin D1 is transcriptionally regulated by and required for transformation by activated signal transducer and activator of transcription 3. *Cancer Res* 66: 2544–2552, 2006.

34. **Li H, Findlay IA, Sheppard DN.** The relationship between cell proliferation, Cl⁻ secretion, and renal cyst growth: a study using CFTR inhibitors. *Kidney Int* 66: 1926–1938, 2004.

35. **Li X, Magenheimer BS, Xia S, Johnson T, Wallace DP, Calvet JP, Li R.** A tumor necrosis factor-alpha-mediated pathway promoting autosomal dominant polycystic kidney disease. *Nat Med* 14: 863–868, 2008.

36. **Liang G, Shao L, Wang Y, Zhao C, Chu Y, Xiao J, Zhao Y, Li X, Yang S.** Exploration and synthesis of curcumin analogs with improved structural stability both in vitro and in vivo as cytotoxic agents. *Bioorg Med Chem* 17: 2623–2631, 2009.

37. **Liby K, Risingsong R, Royce DB, Williams CR, Ma T, Yore MM, Sporn MB.** Triterpenoids CDDO-methyl ester or CDDO-ethyl amide and rexinoids LG100268 or NRX194204 for prevention and treatment of lung cancer in mice. *Cancer Prev Res (Phila Pa)* 2: 1050–1058, 2009.

38. **Liby K, Risingsong R, Royce DB, Williams CR, Yore MM, Honda T, Gribble GW, Lamph WW, Vannini N, Sogno I, Albini A, Sporn MB.** Prevention and treatment of experimental estrogen receptor-negative mammary carcinogenesis by the synthetic triterpenoid CDDO-methyl Ester and the rexinoid LG100268. *Clin Cancer Res* 14: 4556–4563, 2008.

39. **Liby KT, Yore MM, Sporn MB.** Triterpenoids and rexinoids as multifunctional agents for the prevention and treatment of cancer. *Nat Rev Cancer* 7: 357–369, 2007.

40. **Ma Z, Shayeganpour A, Brocks DR, Lavasanifar A, Samuel J.** High-performance liquid chromatography analysis of curcumin in rat plasma: application to pharmacokinetics of polymeric micellar formulation of curcumin. *Biomed Chromatogr* 21: 546–552, 2007.

41. **Magenheimer BS, St John PL, Isom KS, Abrahamson DR, De Lisle RC, Wallace DP, Maser RL, Grantham JJ, Calvet JP.** Early embryonic renal tubules of wild-type and polycystic kidney disease kidneys respond to cAMP stimulation with cystic fibrosis transmembrane conductance regulator/Na⁺,K⁺,2Cl⁻ cotransporter-dependent cystic dilation. *J Am Soc Nephrol* 17: 3424–3437, 2006.

42. **Mochizuki T, Wu G, Hayashi T, Xenophontos SL, Veldhuisen B, Saris JJ, Reynolds DM, Cai Y, Gabow PA, Pierides A, Kimberling WJ, Breuning MH, Constantinou Deltas C, Peters DJM, Somlo S.** PKD2, a gene for polycystic kidney disease that encodes an integral membrane protein. *Science* 272: 1339–1342, 1996.

43. **Nauli SM, Alenghat FJ, Luo Y, Williams E, Vassilev P, Li X, Elia AE, Lu W, Brown EM, Quinn SJ, Ingber DE, Zhou J.** Polycystins 1 and 2 mediate mechanosensation in the primary cilium of kidney cells. *Nat Genet* 33: 129–137, 2003.

44. **Patel V, Li L, Cobo-Stark P, Shao X, Somlo S, Lin F, Igarashi P.** Acute kidney injury and aberrant planar cell polarity induce cyst formation in mice lacking renal cilia. *Hum Mol Genet* 17: 1578–1590, 2008.

45. **Perico N, Antiga L, Caroli A, Ruggenenti P, Fasolini G, Cafaro M, Ondei P, Rubis N, Diadei O, Gherardi G, Prandini S, Panozo A, Bravo RF, Carminati S, Leon FR, Gaspari F, Cortinovis M, Motterlini N, Ene-Iordache B, Remuzzi A, Remuzzi G.** Sirolimus therapy to halt the progression of ADPKD. *J Am Soc Nephrol* 21: 1031–1040, 2010.

46. **Peters DJM, Sandkuijl LA.** Genetic heterogeneity of polycystic kidney disease in Europe. In: *Contributions to Nephrology, Vol 97: Polycystic Kidney Disease*, edited by Breuning MH, Devoto M, and Romeo G. Basel: Karger, 1992, p. 128–139.

47. **Petronelli A, Pannitteri G, Testa U.** Triterpenoids as new promising anticancer drugs. *Anticancer Drugs* 20: 880–892, 2009.

48. **Qian FJ, Watnick TJ, Onuchic LF, Germino GG.** The molecular basis of focal cyst formation in human autosomal dominant polycystic kidney disease. *Cell* 87: 979–987, 1996.

49. **Regis G, Pensa S, Boselli D, Novelli F, Poli V.** Ups and downs: the STAT1:STAT3 seesaw of interferon and gp130 receptor signaling. *Semin Cell Dev Biol* 19: 351–359, 2008.

50. **Ryu K, Choy E, Yang C, Susa M, Hornicek FJ, Mankin H, Duan Z.** Activation of signal transducer and activator of transcription 3 (Stat3) pathway in osteosarcoma cells and overexpression of phosphorylated-Stat3 correlates with poor prognosis. *J Orthop Res* 28: 971–978, 2010.

51. **Saburi S, Hester I, Fischer E, Pontoglio M, Eremina V, Gessler M, Quaggin SE, Harrison R, Mount R, McNeill H.** Loss of Fat4 disrupts PCP signaling and oriented cell division and leads to cystic kidney disease. *Nat Genet* 40: 1010–1015, 2008.

52. **Scheper MA, Nikitakis NG, Sauk JJ.** Survivin is a downstream target and effector of sulindac-sensitive oncogenic Stat3 signaling in head and neck cancer. *Int J Oral Maxillofac Surg* 36: 632–639, 2007.

53. **Serra AL, Poster D, Kistler AD, Krauer F, Raina S, Young J, Rentsch KM, Spanaus KS, Senn O, Kristanto P, Scheffel H, Weishaupt D, Wuthrich RP.** Sirolimus and kidney growth in autosomal dominant polycystic kidney disease. *N Engl J Med* 363: 820–829, 2010.

54. **Sharif-Naeini R, Folgering JHA, Bichet D, Duprat F, Lauritzen I, Arhatte M, Jodar M, Dedman A, Chatelain F, Schulte U, Loufrani F, Patel A, Sachs F, Delmas P, Peters DJM, Honore E.** Polycystin-1 and -2 dosage regulates pressure sensing. *Cell* 109: 587–596, 2009.

55. **Shillingford JM, Murcia NS, Larson CH, Low SH, Hedgepeth R, Brown N, Flask CA, Novick AC, Goldfarb DA, Kramer-Zucker A, Walz G, Piontek KB, Germino GG, Weimbs T.** The mTOR pathway is regulated by polycystin-1, and its inhibition reverses renal cystogenesis in polycystic kidney disease. *Proc Natl Acad Sci USA* 103: 5466–5471, 2006.

56. **Shillingford JM, Piontek KB, Germino GG, Weimbs T.** Rapamycin ameliorates PKD resulting from conditional inactivation of Pkd1. *J Am Soc Nephrol* 21: 489–497, 2010.

57. **Singletary K, MacDonald C, Iovinelli M, Fisher C, Wallig M.** Effect of the beta-diketones diferuloylmethane (curcumin) and dibenzoylmethane on rat mammary DNA adducts and tumors induced by 7,12-dimethylbenz[a]anthracene. *Carcinogenesis* 19: 1039–1043, 1998.

58. **Strimpakos AS, Sharma RA.** Curcumin: preventive and therapeutic properties in laboratory studies and clinical trials. *Antioxid Redox Signal* 10: 511–545, 2008.

59. **Swamy MV, Citineni B, Patlolla JM, Mohammed A, Zhang Y, Rao CV.** Prevention and treatment of pancreatic cancer by curcumin in combination with omega-3 fatty acids. *Nutr Cancer* 60, Suppl 1: 81–89, 2008.

60. **Takakura A, Contrino L, Zhou X, Bonventre JV, Sun Y, Humphreys BD, Zhou J.** Renal injury is a third hit promoting rapid development of adult polycystic kidney disease. *Hum Mol Genet* 18: 2523–2531, 2009.

61. **Tao Y, Kim J, Schrier RW, Edelstein CL.** Rapamycin markedly slows disease progression in a rat model of polycystic kidney disease. *J Am Soc Nephrol* 16: 46–51, 2005.

62. **The European Polycystic Kidney Disease Consortium, Ward CJ, Peral B, Hughes J, Thomas S, Gamble V, MacCarthy A, Sloane-Stanley J, Buckle V, Kearney LHD, Ratcliffe P, Harris P, Roelfsema J, Spruit L, Saris J, Dauwerse H, Peters D, Breuning M, Nellist M, Brook-Carter P, Maheshwar M, Cordeiro I, Santos H, Cabral P, Sampson J, Janssen B, Hesseling-Janssen A, van den Ouweland AM, Eussen B, Verhoef S, Lindhout D, Halley D.** The polycystic kidney disease 1 gene encodes a 14 kb transcript and lies within a duplicated region on chromosome 16. *Cell* 77: 881–894, 1994.

63. **Torres VE.** Vasopressin antagonists in polycystic kidney disease. *Kidney Int* 68: 2405–2418, 2005.

64. **Torres VE, Harris PC.** Mechanisms of disease: autosomal dominant and recessive polycystic kidney diseases. *Nat Clin Pract Nephrol* 2: 40–55, 2006.

65. **Torres VE, Wang X, Qian Q, Somlo S, Harris PC, Gattone VH.** Effective treatment of an orthologous model of autosomal dominant polycystic kidney disease. *Nat Med* 10: 363–364, 2004.

66. **Walz G, Budde K, Mannaa M, Nurnberger J, Wanner C, Sommerer C, Kunzendorf U, Banas B, Horl WH, Obermuller N, Arns W, Pavenstadt H, Gaedeke J, Buchert M, May C, Gschaidmeier H, Kramer S, Eckardt KU.** Everolimus in patients with autosomal dominant polycystic kidney disease. *N Engl J Med* 363: 830–840, 2010.

67. **Wilson PD.** Polycystic kidney disease. *N Engl J Med* 350: 151–164, 2004.

68. **Wu G, D'Agati V, Cai Y, Markowitz G, Park JH, Reynolds DM, Maeda Y, Le TC, Hou H Jr, Kucherlapati R, Edelmann W, Somlo S.** Somatic inactivation of Pkd2 results in polycystic kidney disease. *Cell* 93: 177–188, 1998.

69. **Yamaguchi T, Nagao S, Wallace DP, Belibi FA, Cowley BD, Pelling JC, Grantham JJ.** Cyclic AMP activates B-Raf and ERK in cyst epithelial cells from autosomal-dominant polycystic kidneys. *Kidney Int* 63: 1983–1994, 2003.